CrystEngComm

PAPER

View Article Online
View Journal | View Issue

Cite this: *CrystEngComm*, 2025, **27**, 3552

Diverse tetracyanodihydrodipyrazinopyrazine clathrate crystals assembled from weak intermolecular interactions†

Kosuke Watanabe, [ab] Haruki Sugiyama[abcd] and Yasutomo Segawa *[ab]

Received 15th March 2025,
Accepted 23rd April 2025

DOI: 10.1039/d5ce00289c

rsc.li/crystengcomm

Tetracyanodihydrodipyrazinopyrazines with two mesityl (2,4,6-trimethylphenyl) groups formed clathrate crystals with 15 kinds of organic solvents. Two common types of host molecular networks were observed in the crystals. Theoretical calculations indicated that these host networks are constructed from π–π and CN–π interactions. As these intermolecular interactions are relatively weak, the host network can change flexibly in response to guest molecules. Guest-free crystals can be reversibly transformed into clathrate crystals through crystal-to-crystal phase transitions *via* the adsorption/desorption of solvent vapor.

Introduction

Clathrate crystals are a class of inclusion crystals in which the host molecules or host molecular network (host network) encapsulates guest molecules *via* non-covalent interactions to form stabilized structures.[1] Clathrate crystals have attracted significant attention owing to their potential applications that use their selective molecular recognition and inclusion abilities in separators and reservoirs of chemical substances.[2] The formation of clathrate crystals has been used as a crystal-engineering technique in the pharmaceutical industry and in materials science to modify crystal structures through host–guest interactions. Various solid-state properties such as the melting point and dissolution rate, as well as optical and electronic properties, can be tuned by the structural modification of the host molecules.[3]

Rigid and bulky molecules tend to form clathrate crystals because guest-free close packing is inhibited. Several molecular structures, such as wheel-and-axle shaped, scissor-like, and roof-shaped structures, have been proposed as suitable hosts of clathrate crystals.[4] The typical interactions that exist between the host molecules in such clathrate crystals are van der Waals forces and hydrogen bonds.[5] Clathrate crystals exhibit structural flexibility and reversibility because the host networks are formed by relatively weak and reversible interactions. The properties of the networks vary significantly depending on the types of interactions involved.

For example, 9,10-diphenylanthracene (DPA) is a rigid host molecule that has been investigated for its tunable physical properties. DPA is a scissor-like molecule with a rigid anthracene core and two phenyl groups that are twisted from the anthracene plane due to steric repulsion. DPA can form clathrate crystals with 1,4-dioxane, hexafluorobenzene, tetrachloroethane, polycyclic arenes, and fullerene *via* van der Waals interactions.[6] DPA derivatives have also been used as host molecules of hydrogen-bonded networks that incorporate guest molecules such as esters and ketones.[7] However, DPA-based clathrate crystals that use dipole–dipole interactions have not been actively investigated, even though they have the potential to provide a novel strategy for the molecular design of clathrate crystals and host molecules.

Previously, we developed the synthesis and three-dimensional (3D) polymerization of 2,3,7,8-tetracyano-5,10-dihydrodipyrazino[2,3-*b*:2′,3′-*e*]pyrazine (TCDP), which bears two mesityl (2,4,6-trimethylphenyl) groups at the 5,10-positions (Fig. 1).[8] Due to the steric hindrance arising from the methyl

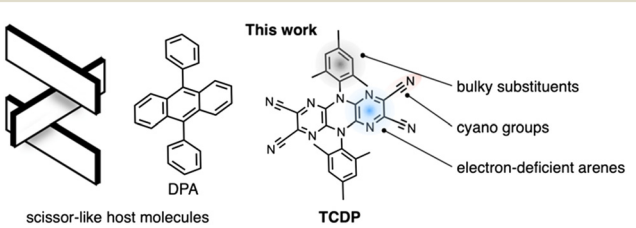

Fig. 1 Scissor-like host molecules DPA and TCDP.

[a] *Institute for Molecular Science, Myodaiji, Okazaki, 444-8787, Japan. E-mail: segawa@ims.ac.jp*
[b] *The Graduate University for Advanced Studies, SOKENDAI, Myodaiji, Okazaki, 444-8787, Japan*
[c] *Neutron Industrial Application Promotion Center, Comprehensive Research Organization for Science and Society, Tokai, Ibaraki 319-1106, Japan*
[d] *Department of Chemistry, School of Science, Institute of Science Tokyo, 2-12-1, Ookayama, Meguro, Tokyo, Japan*

† Electronic supplementary information (ESI) available: Experimental and computational details (PDF). CCDC 2429929–2429944 and 2431197. For ESI and crystallographic data in CIF or other electronic format see DOI: https://doi.org/10.1039/d5ce00289c

groups, the mesityl groups are arranged nearly perpendicular to the central π-plane, thus forming a scissor-like structure similar to DPA. In addition to the molecular structure of TCDP, the electron-deficient aromatic core and four cyano groups are expected to enhance the formation of host networks through multi-directional intermolecular interactions. Herein, we report the formation of diverse clathrate crystals using TCDP as a host molecule. Furthermore, we have analyzed the dependence of the host network structures on the type of guest molecule using computational chemistry methods. TCDP was found to form various clathrate crystals with various organic solvents. These clathrate crystals exhibit two types of host–host interaction motifs: π–π stacking interactions between parallel dicyanopyrazine molecules and CN–π interactions involving the lone pair of the cyano groups oriented toward the pyrazine rings. The crystal structures of the clathrate crystals were classified systematically based on their interaction motifs and dimensionality, and energy calculations were performed for the two interaction motifs. Subsequently, the adsorption capabilities of the homomolecular crystals were examined by exposing them to organic-solvent vapor. The desorption behavior of the clathrate crystals was investigated using thermogravimetry in combination with differential thermal analysis (TG-DTA).

Results and discussion

Homomolecular TCDP crystals

Homomolecular crystals of TCDP (**HC-TCDP**) were obtained by sublimation at 300 °C under *ca.* 0.1 Torr and the solid-state structure was analyzed using X-ray crystallography at −130 °C. As shown in Fig. 2a and b, the crystal structure exhibited π–π stacking interactions between the dicyanopyrazine units with a stacking distance of 3.4082(7) Å. Notably, the crystal has unoccupied voids with a calculated volume of 87.29 Å^3 per cell (12.4% of the unit cell, probe radius: 1.2 Å; Fig. 2c). The two mesityl groups were arranged almost perpendicular to the central π-plane owing to steric hindrance. The recrystallization of TCDP from (*R*)-(+)-limonene or (1*R*)-(+)-pinene afforded the same crystal structure as for **HC-TCDP**. The rigid and bulky structure of TCDP seems to hinder dense packing, resulting in the formation of the voids in the crystal structure. TCDP was therefore expected to form clathrate crystals by filling these voids with solvent molecules.

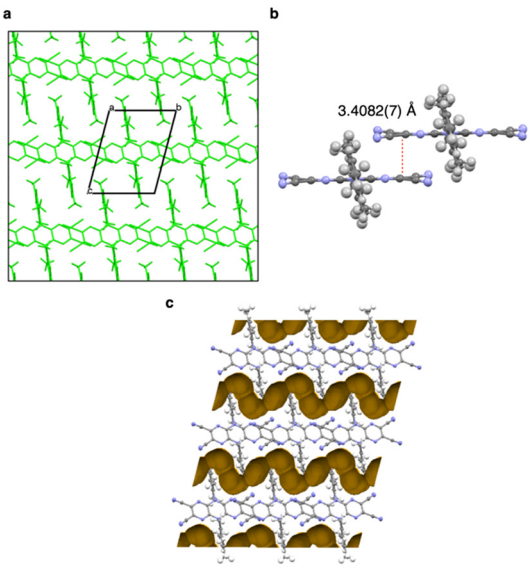

Fig. 2 (a) Crystal structure of **HC-TCDP**. (b) Crystal packing of **TCDP·SF**. (c) Voids in the **HC-TCDP** crystal highlighted in brown.

Clathrate crystals bearing π–π host networks

TCDP was found to form clathrate crystals with various organic solvent molecules. The recrystallization of TCDP from tetrahydrofuran (THF), *N*,*N*-dimethylformamide (DMF), acetone, diphenyl ether (Ph_2O), benzene, or thiophene yielded the corresponding clathrate crystals **TCDP·THF**, **TCDP·DMF**, **TCDP·acetone**, **TCDP·Ph_2O**, **TCDP·benzene**, and **TCDP·thiophene**. The host networks of **TCDP·THF** (Fig. 3c) and **TCDP·DMF** (Fig. 3e) are isostructural to **TCDP·acetone** (Fig. 3a), whereas **TCDP·benzene** and **TCDP·thiophene** are isostructural to each other (Fig. 4c and e). The two-dimensional (2D) host networks are formed *via* π–π interactions between the dicyanopyrazine units and weak dispersion forces between the mesityl groups.

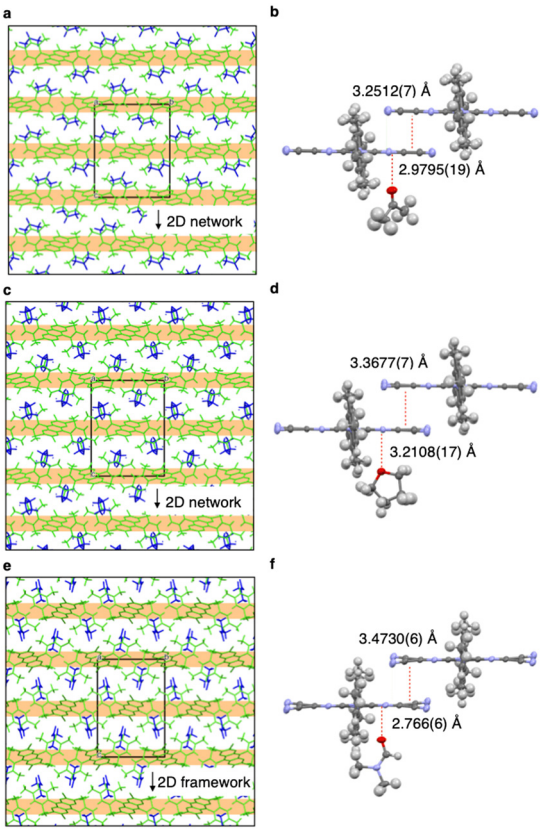

Fig. 3 (a) Crystal structure of **TCDP·acetone**. (b) Crystal packing of **TCDP·acetone**. (c) Crystal structure of **TCDP·THF**. (d) Crystal packing of **TCDP·THF**. (e) Crystal structure of **TCDP·DMF**. (f) Crystal packing of **TCDP·DMF**.

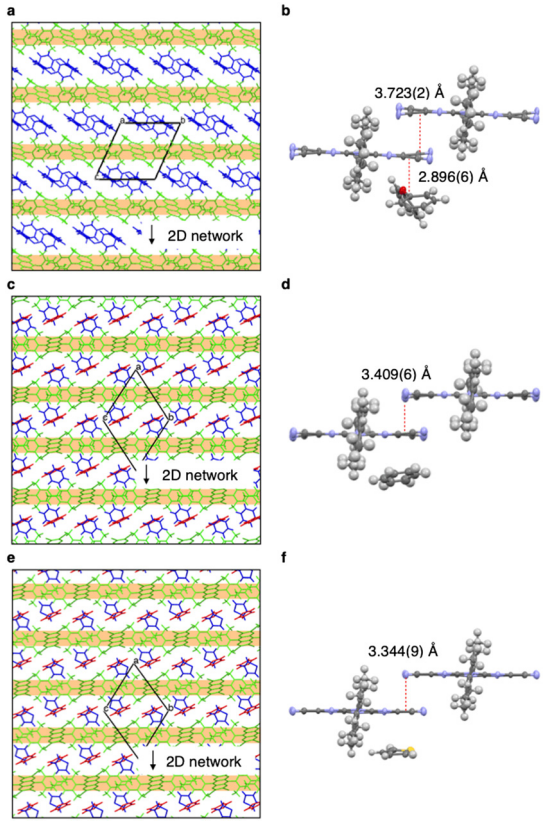

Fig. 4 (a) Crystal structure of **TCDP·Ph$_2$O**. (b) Crystal packing of **TCDP·Ph$_2$O**. (c) Crystal structure of **TCDP·benzene**. (d) Crystal packing of **TCDP·benzene**. (e) Crystal structure of **TCDP·thiophene**. (f) Crystal packing of **TCDP·thiophene**.

TCDP·acetone, **TCDP·THF**, and **TCDP·DMF** exhibit host–guest ratios of 1 : 2. The π–π distances between the host molecules in **TCDP·acetone**, **TCDP·THF**, and **TCDP·DMF** are 3.2512(7), 3.3677(7), and 3.4730(6) Å, respectively (Fig. 3b, d, and f). The oxygen atoms of the acetone, THF, and DMF molecules are directed toward the pyrazine rings of the host molecules, where the oxygen–pyrazine distances are 2.9795(19) (**TCDP·acetone**), 3.2108(17) (**TCDP·THF**), and 2.766(6) Å (**TCDP·DMF**). **TCDP·Ph$_2$O** also shows a host–guest ratio of 1 : 2 (Fig. 4a), and alternating layers of TCDP and Ph_2O are observed in the crystal structure, wherein the π–π stacking distance between the host molecules is 3.723(2) Å (Fig. 4b). The oxygen atoms of the Ph_2O molecules are also directed toward the pyrazine rings of TCDP (oxygen–pyrazine distance = 2.896(6) Å), which can be recognized as lone pair–π interactions. **TCDP·benzene** and **TCDP·thiophene** exhibit host–guest ratios of 1 : 4 (Fig. 4c and e) and the guest solvent layers are embedded between the 2D host network layers. The host molecules are stacked with a horizontal shift *via* π–π interactions with a stacking distance of 3.409(6) Å (**TCDP·benzene**) and 3.344(9) Å (**TCDP·thiophene**) (Fig. 4d and f). Here, the guest molecules interact with the mesityl groups through weak CH–π interactions.

To further investigate the π–π host networks, we explored the formation of clathrate crystals with other solvents. Recrystallization from chlorobenzene (PhCl), iodobenzene (PhI), and ethyl acetate (EtOAc) yielded the corresponding clathrate crystals **TCDP·PhCl**, **TCDP·PhI**, and **TCDP·EtOAc**. These crystals form 1D π–π host networks, whereby **TCDP·PhCl** and **TCDP·PhI** are isostructural to each other. **TCDP·PhCl** and **TCDP·PhI** exhibit host–guest ratios of 1 : 1, whereby the guest molecules interact with the mesityl groups of the host molecules. The 1D channels filled with solvent molecules are arranged perpendicularly to the 1D network formed by TCDP (Fig. 5a and c). As shown in Fig. 5b and d, the stacking distances between the host molecules in **TCDP·PhCl** and **TCDP·PhI** are 3.4320(11) and 3.4849(10) Å, respectively. On the other hand, **TCDP·EtOAc**, which exhibits a host–guest ratio of 1 : 2, exhibits a complicated structure when compared to **TCDP·PhCl** and **TCDP·PhI**. The 1D channels filled with ethyl acetate adopt an arrangement parallel to the 1D host networks (Fig. 5e). As shown in Fig. 5f, the carbonyl oxygen atoms of both ethyl acetate molecules are oriented toward the pyrazine rings with oxygen–pyrazine distances of 2.990(5) and 2.991(4) Å.

The clathrate crystals **TCDP·pyridine** and **TCDP·DCM**, obtained from pyridine and dichloromethane (DCM), respectively, exhibit 3D host networks. The 3D host network of **TCDP·pyridine** is formed *via* π–π stacking interactions between the dicyanopyrazine units, and weak dispersion forces in two directions (Fig. 6a). Here, the host–guest ratio is 1 : 2, and the

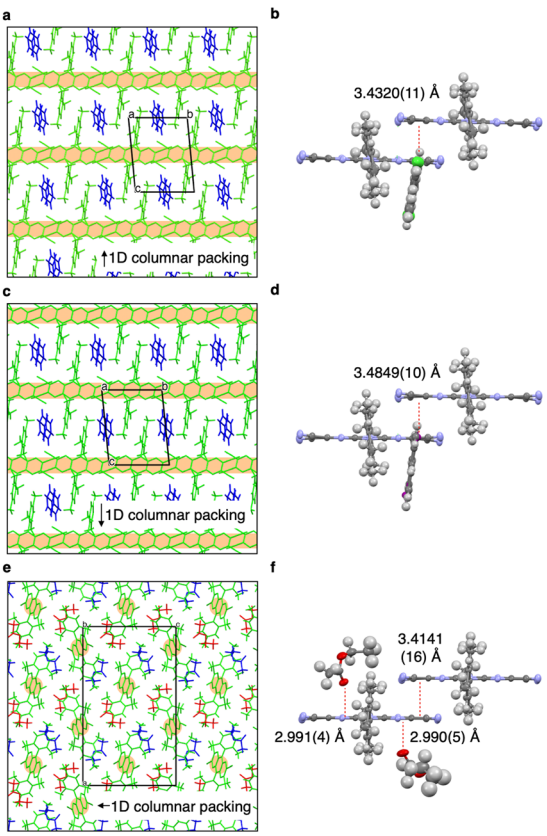

Fig. 5 (a) Crystal structure of **TCDP·PhCl**. (b) Crystal packing of **TCDP·PhCl**. (c) Crystal structure of **TCDP·PhI**. (d) Crystal packing of **TCDP·PhI**. (e) Crystal structure of **TCDP·EtOAc**. (f) Crystal packing of **TCDP·EtOAc**.

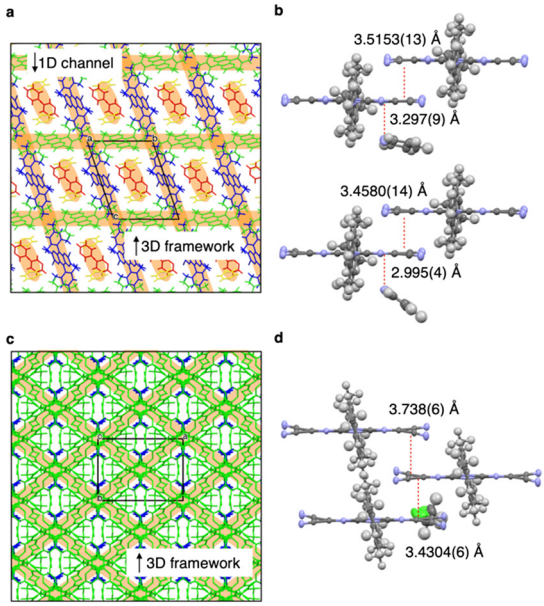

Fig. 6 (a) Crystal structure of **TCDP·pyridine**. (b) Crystal packing of **TCDP·pyridine**. (c) Crystal structure of **TCDP·DCM**. (d) Crystal packing of **TCDP·DCM**.

presence of pyridine-filled 1D channels that penetrate the 3D host network was noted. The stacking distances between the host molecules are 3.5153(13) and 3.4580(14) Å, and the nitrogen atoms of the pyridine molecules are located 3.297(9) and 2.995(4) Å away from the pyrazine ring (Fig. 6b). On the other hand, **TCDP·DCM** has a host–guest ratio of 1 : 1 and forms a 3D host network based on π–π stacking interactions in two directions and dispersion forces in one direction (Fig. 6c). The stacking distance between the host molecules is 3.4304(6) Å, and DCM is isolated and included in the space surrounded by TCDP (Fig. 6d). No significant intermolecular interactions were observed between DCM and the host molecules.

Clathrate crystals that bear CN–π host networks

The formation of CN–π host networks induced by lone pair–π interactions was explored by creating this type of clathrate crystal. Recrystallization from 1,2-dichloroethane (DCE) yielded clathrate crystal **TCDP·DCE**, which is isostructural to **TCDP·MeCN** (MeCN: acetonitrile) (Fig. 7a and c). As shown in Fig. 7b and d, the host molecules in **TCDP·MeCN** and **TCDP·DCE** are linked by interactions between the cyano groups and the pyrazine rings, with distances of 2.965(2) and 3.0471(18) Å, respectively. Moreover, the MeCN and DCE molecules are oriented toward the cyano groups of TCDP, with distances of 3.1061(14) and 3.738(10) Å, respectively. As shown in Fig. 7e, the 2D networks are linked *via* cyclic intermolecular interactions that involve four TCDP molecules. Here, the crystal structure shows that the guest molecules are surrounded by TCDP.

To further explore solvents for the creation of CN–π host networks, we examined the isostructural 3D network structures

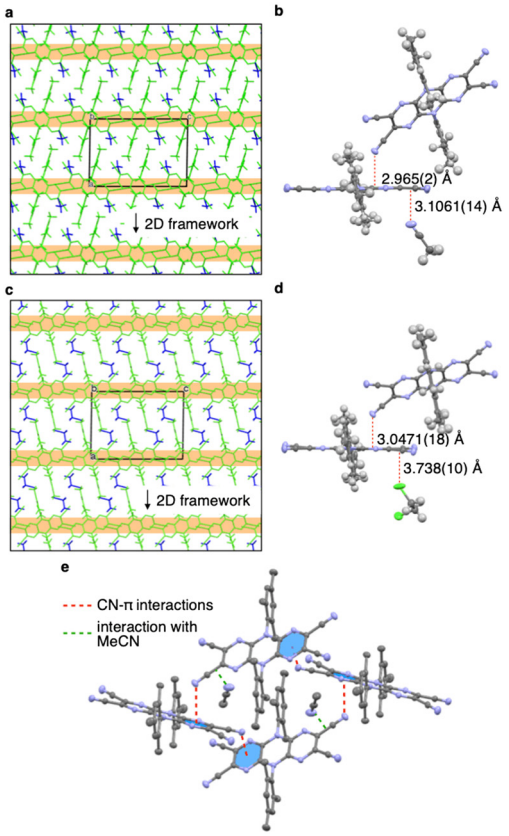

Fig. 7 (a) Crystal structure of **TCDP·MeCN**. (b) Crystal packing of **TCDP·MeCN**. (c) Crystal structure of **TCDP·DCE**. (d) Crystal packing of **TCDP·DCE**. (e) Cyclic interaction motif of four **TCDP** molecules in **TCDP·MeCN**.

with 1 : 1 host–guest ratios of toluene (PhMe) and *ortho*-dichlorobenzene (ODCB) clathrate crystals (**TCDP·PhMe** and **TCDP·ODCB**; Fig. 8a and c). Their networks consist of cyclic intermolecular CN–π interactions that involve six host molecules (Fig. 8e). The cyano-pyrazine distances in **TCDP·PhMe** and **TCDP·ODCB** are 2.9278(16), 3.3813(18), and 3.1227(15) Å and 3.000(3), 3.371(3), and 3.166(4) Å, respectively (Fig. 8b and d). Their crystal structures show that the solvent molecules are encapsulated by the host molecules.

Classification of TCDP clathrate crystals according to the host networks

As shown in Fig. 9, the 15 obtained crystal structures were classified according to the following criteria: i) intermolecular interactions and ii) dimensionality of the host networks. Table S5† summarizes the intermolecular interactions between the host molecules, the dimensionality of the host networks, the host–guest ratios, and the space groups of the clathrate crystals.

Understanding the intermolecular interactions through theoretical calculations

Intermolecular host–host and host–guest interactions were analyzed using computational-chemistry techniques to elucidate

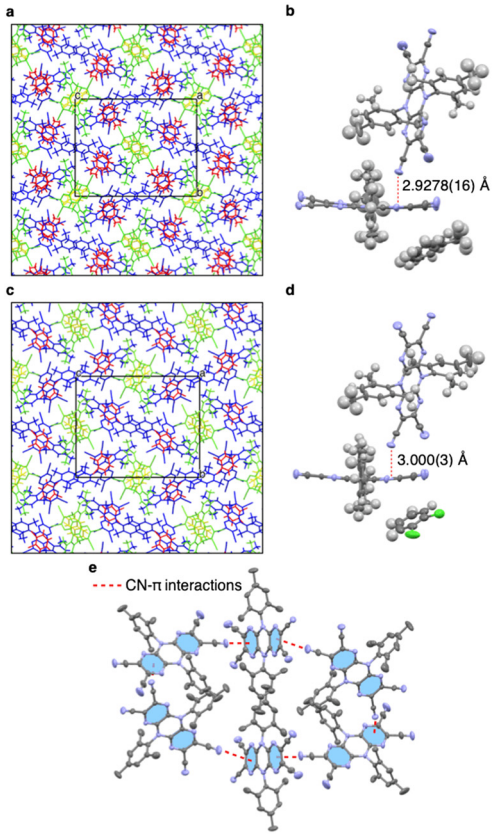

Fig. 8 (a) Crystal structure of **TCDP·PhMe**. (b) Crystal packing of **TCDP·PhMe**. (c) Crystal structure of **TCDP·ODCB**. (d) Crystal packing of **TCDP·ODCB**. (e) Cyclic interaction of six **TCDP** molecules in **TCDP·PhMe**.

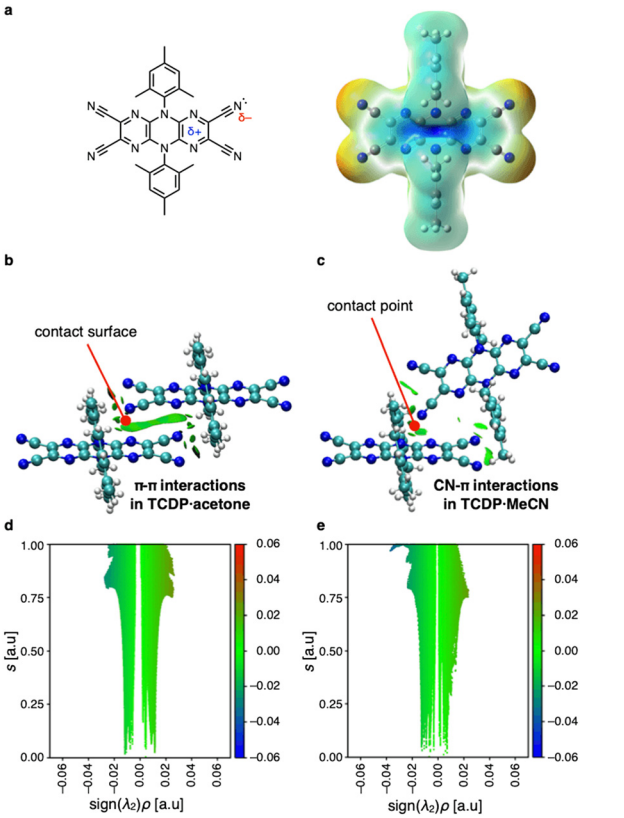

Fig. 10 (a) Electrostatic potential map of TCDP. (b) NCI plots of π–π interactions in **TCDP·acetone** and (c) CN–π interactions in **TCDP·MeCN**. An isosurface value of 0.3 a.u. was applied to the structure. (d and e) Plot of *s vs.* sign(λ_2)ρ for **TCDP·acetone** (d) and **TCDP·MeCN** (e). A large, negative value of sign(λ_2)ρ indicates an attractive interaction, while a large, positive value reflects strong non-bonding overlap.

the mechanism of the host-network formation and the guest inclusion. Using Gaussian16,[9] an electrostatic potential map was generated at the B3LYP/6-31G(d) level (Fig. 10a).[10,11] The results revealed that the nitrogen atoms of the cyano groups were negatively charged and that the pyrazine rings were positively charged. This was attributed to the polarization of the cyano groups, the presence of a lone pair of electrons on the nitrogen atoms, and the electron-deficient nature of the pyrazine rings. Non-covalent interaction (NCI) plots[12,13] were generated for **TCDP·acetone** and **TCDP·MeCN** (Fig. 10b and c). In both systems, green isosurfaces were observed, indicating regions of π–π interactions between the dicyanopyrazine units in **TCDP·acetone**, and a CN–π interaction between the cyano group and pyrazine ring in **TCDP·MeCN**. Both interactions are very weak, as reflected in the sign(λ_2)ρ values, which range from −0.03 to 0.03 a.u. (Fig. 10d and e).

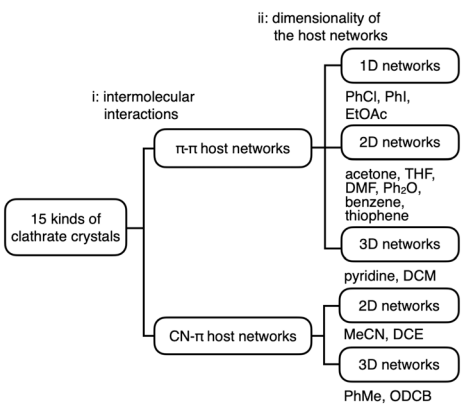

Fig. 9 Classification of the 15 TCDP clathrate crystals.

Crystal Explorer[14] was used to analyze the contributions of intermolecular interactions to the π–π host networks (**TCDP·EtOAc**, **TCDP·acetone**, and **TCDP·benzene**) and CN–π host networks (**TCDP·MeCN** and **TCDP·DCE**). As shown in Table S3,† the results revealed that electrostatic interactions contribute to both types of networks. These interactions are primarily driven by dipole–dipole interactions and lone pair–π interactions. The contribution of electrostatic interactions to the host network in **TCDP·benzene** was relatively small compared to other clathrates, which might be attributed to offsets in the π–π host networks. Electrostatic interactions between the host and guest molecules, particularly lone pair–π interactions, contribute significantly to the host networks in **TCDP·EtOAc**, **TCDP·acetone**, and

TCDP·MeCN, which all have polar functional groups. On the other hand, dispersion forces predominate in **TCDP·benzene** and **TCDP·DCE**.

Vapor-induced formation of clathrate crystals

Given that the host networks of the obtained clathrate crystals were constructed by weak interactions, the structures (or host networks) are expected to be able to change flexibly to accommodate guest molecules. We attempted the transition of homomolecular crystal **HC-TCDP** to clathrate crystals by exposing it to solvent vapor. First, we found that desolvation of **TCDP·benzene** at 100 °C under reduced pressure took place and the powder X-ray diffraction (PXRD) patterns of the thus-obtained desolvated crystals are in good agreement with the simulated pattern from X-ray crystallography of **HC-TCDP** measured at room temperature (Fig. 11a). Then, as depicted in Fig. 11b, the desolvated crystals were exposed to solvent vapor for 3 days. Exposure to the vapor resulted in the vapor-induced formation of clathrate crystals, with the exceptions of benzene, thiophene, DCM, DCE, and Ph_2O (Fig. S1†). Fig. 11c and d show representative examples of the changes in the PXRD patterns before and after exposure to acetone and MeCN. The PXRD patterns obtained after vapor exposure are consistent with those of the corresponding clathrate crystals prepared by recrystallization. Therefore, **HC-TCDP** can be stimulated to form clathrate crystals by exposure to solvent vapor. Although **HC-TCDP** exhibits a π–π host network, CN–π-type clathrate crystals **TCDP·MeCN**, **TCDP·PhMe**, and **TCDP·ODCB** could still be obtained upon exposure to vapor. These results indicate that the relatively weak interactions between the dicyanopyrazine units favor dynamic molecular rearrangement through the formation of clathrate crystals. On the other hand, neither benzene nor thiophene exhibited adsorption behavior or crystal structure changes; the crystal structures of **TCDP·benzene** and **TCDP·thiophene** are isomorphic, with alternating layers of solvent and TCDP. Furthermore, the results of the interaction calculations suggest that the stabilization energy is small and that this layered structure is not favorable for adsorption. Solvent desorption from **TCDP·benzene** occurred within 1 minute under atmospheric conditions (Fig. S2†). For DCM or DCE, a slurry-like substance was formed and PXRD measurements were not possible. This could be due to organic-vapor-induced dissolution caused by the high vapor pressure of these solvents.

Guest-molecule-desorption behavior

TG-DTA analyses were performed to study the solvent-desorption behavior from the clathrate crystals in detail. The clathrate crystals, which were obtained in sufficient volume following solvent-vapor exposure, were subsequently subjected to a TG-DTA analysis. All clathrate crystals exhibited one-step solvent desorption processes, whereby the weight loss was in good agreement (~1% error) with the theoretically expected values (Fig. 12a and c and S3, as well as Table S6†), and the PXRD patterns obtained after desorption agreed with the simulated one from **HC-TCDP** measured at room temperature (Fig. 12b and d and S4†). As shown in Fig. 12a and c, acetone and MeCN desorbed at 92.4 and 78.5 °C, respectively, whereby the desorption temperature of acetone is above its boiling point due to stabilization within the clathrate crystals. EtOAc desorbed very quickly at 65 °C, suggesting an effect caused by the crystal solvent present in the 1D channels (Fig. 5e and S3†). Although the aromatic solvents (PhCl, PhI, PhMe, ODCB) have similar vapor pressures and boiling points, and even though the host–guest-interaction analyses indicated similar interactions within each clathrate crystal, the desorption temperatures for PhMe and ODCB are much higher than for

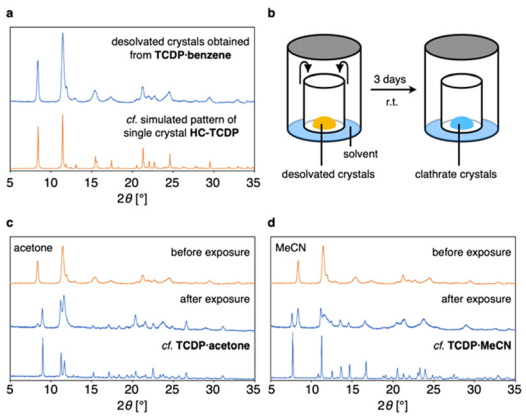

Fig. 11 (a) PXRD patterns of the desolvated crystals of **TCDP·benzene**, and a PXRD pattern simulated from the single crystal X-ray diffraction of **HC-TCDP** measured at room temperature. (b) Schematic diagram of the solvent-vapor-exposure experiment. (c and d) Results of the vapor-exposure experiment with acetone (c) and MeCN (d).

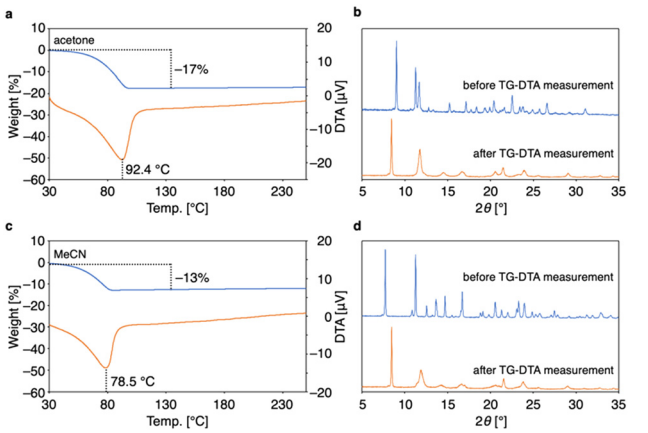

Fig. 12 (a) TG-DTA curves of **TCDP·acetone**. (b) PXRD patterns of **TCDP·acetone** before and after the TG-DTA measurement. (c) TG-DTA curves of **TCDP·MeCN**. (d) PXRD patterns of **TCDP·MeCN** before and after the TG-DTA measurement.

PhCl and PhI. The PhCl and PhI molecules are aligned to form 1D channels, whereas PhMe and ODCB are encapsulated in the network of their crystal structures. The former clathrate crystal structures can thus be expected to be preferable for guest-molecule desorption compared to the latter. The difference in crystal packing also affects the desorption temperature (Fig. 5a and c and 8a and c and S3†); the TG curve of **TCDP·acetone** (Fig. 12a) suggests that acetone guest molecules begin to desorb at around room temperature. To monitor the desorption behavior under ambient conditions, time-dependent PXRD measurements under atmospheric conditions at room temperature were performed on **TCDP·acetone**. As shown in Fig. S5,† the PXRD pattern of **TCDP·acetone** gradually decayed and simultaneously changed to match that of **HC-TCDP**. This change of the PXRD pattern indicates a crystal-to-crystal phase transition from **TCDP·acetone** to **HC-TCDP**.

Conclusions

In this study, we generated 15 different clathrate crystals of 2,3,7,8-tetracyano-5,10-dihydrodipyrazino[2,3-*b*,2′,3′-*e*]pyrazine (TCDP) and analyzed their network structures using crystallographic and computational techniques. TCDP is a rigid and bulky molecule with a dipyrazinopyrazine moiety and two mesityl groups that are arranged nearly perpendicular to the π-plane. TCDP provided clathrate crystals *via* recrystallization from 15 kinds of organic solvents. π–π and CN–π host networks were observed in the crystal structures, whereby the former is based on π–π interactions and the latter on CN–π interactions between the dicyanopyrazine moieties. An analysis of the intermolecular interactions using theoretical calculations indicated that dispersion forces and dipole–dipole interactions are the main factors that drive the formation of the host networks. In addition, the pyrazine rings are positively charged and serve as electron acceptor sites for trapping guests with lone pairs of electrons. Adsorption and desorption experiments revealed that the homomolecular TCDP crystal (**HC-TCDP**) and the solvated clathrate crystals are interchangeable. The scissor-like host molecules form flexible CN-based networks that allow adaptable structural changes that can effectively encapsulate a variety of guest molecules, forming stable complexes. The acceptor sites of the pyrazine units and the surrounding mesityl groups facilitate guest inclusion through CH–π interactions. Such flexible and robust networks take advantage of the directional and weak intermolecular interactions of the dicyanopyrazine groups (a relatively rare motif in clathrate crystals), thus demonstrating new principles of molecular design. The approach employed here enables the creation of versatile clathrate crystals with high structural flexibility and stability, and has potential applications in diverse fields such as molecular recognition, gas/liquid storage, sensing, and soft materials.

Data availability

Crystallographic data have been deposited at the CCDC under 2429929–2429944 and 2431197. The data supporting this article are included in the ESI.†

Conflicts of interest

The authors declare no competing financial interests.

Acknowledgements

This work was supported by the FOREST program (JPMJFR211R to Y. S.) from the JST, JSPS KAKENHI grants JP22K19038 and JP22H02068 (to Y. S.), the Murata Science and Education Foundation, and the Foundation of Public Interest of Tatematsu. The authors thank Mr. Yusuke Yagisawa (Yamagata University) for attempted recrystallization. K. W. is a recipient of a JSPS Research Fellowship for Young Scientists (DC1). This work was conducted at the IMS supported by ARIM (JPMXP1224MS5001). Calculations were performed using resources of the Research Center for Computational Science, Okazaki, Japan (24-IMS-C232).

Notes and references

1 (*a*) L. Mandelcorn, *Chem. Rev.*, 1959, **59**, 827–839; (*b*) J. E. Werner and J. A. Swift, *CrystEngComm*, 2021, **23**, 1555–1565; (*c*) D. D. MacNicol, J. J. McKendrick and D. R. Wilson, *Chem. Soc. Rev.*, 1978, **7**, 65–87; (*d*) A. S. Jessiman, D. D. Macnicol, P. R. Mallinson and I. Vallance, *J. Chem. Soc., Chem. Commun.*, 1990, 1619–1621.

2 (*a*) F. Lee, E. Gabe, J. S. Tse and J. A. Ripmeester, *J. Am. Chem. Soc.*, 1988, **110**, 6014–6019; (*b*) J.-P. Torré, R. Coupan, M. Chabod, E. Pere, S. Labat, A. Khoukh, R. Brown, J.-M. Sotiropoulos and H. Gornitzka, *Cryst. Growth Des.*, 2016, **16**, 5330–5338; (*c*) T. Hertzsch, F. Budde, E. Weber and J. Hulliger, *Angew. Chem., Int. Ed.*, 2002, **41**, 2281–2284; (*d*) M. Rahmani, C. R. M. O. Matos, S.-Q. Wang, A. A. Bezrukov, A. C. Eaby, D. Sensharma, Y. Hjiej-Andaloussi, M. Vandichel and M. J. Zaworotko, *J. Am. Chem. Soc.*, 2023, **145**, 27316–27324.

3 (*a*) M. Nowak, A. J. Dyba, J. Janczak, A. Morritt, L. Fabian, B. Karolewicz, Y. Z. Khimyak, D. E. Braun and K. P. Nartowski, *Mol. Pharmaceutics*, 2022, **19**, 456–471; (*b*) A. L. Bingham, D. S. Hughes, M. B. Hursthouse, R. W. Lancaster, S. Tavener and T. L. Threlfall, *Chem. Commun.*, 2001, 603–604; (*c*) K. Sugawara, T. Ono, Y. Yano, T. Suzuki and Y. Ishigaki, *Mater. Chem. Front.*, 2023, **7**, 1591–1598; (*d*) M. Okazaki, Y. Takeda, P. Data, P. Pander, H. Higginbotham, A. P. Monkman and S. Minakata, *Chem. Sci.*, 2017, **8**, 2677–2686.

4 (*a*) P. P. Mazzeo, A. Bacchi and P. Pelagatti, *Coord. Chem. Rev.*, 2020, **414**, 213302; (*b*) E. Weber, in *Inclusion Compounds*, ed. J. L. Atwood, J. E. D. Davies and D. D. MacNicol, Oxford University Press, Oxford, 1991, ch. 5, vol. 4; (*c*) R. Bishop, *Chem. Soc. Rev.*, 1996, **25**, 311–319; (*d*) E. Weber, M. Czugler and I. Goldberg, *Molecular inclusion and molecular recognition – clathrates II*, De Gruyter, Berlin, 1988.

5 (*a*) R.-B. Lin, Y. He, P. Li, H. Wang, W. Zhou and B. Chen, *Chem. Soc. Rev.*, 2019, **48**, 1362–1389; (*b*) H. Yamagishi, H. Sato, A. Hori, Y. Sato, R. Matsuda, K. Kato and T. Aida, *Science*, 2018, **361**, 1242–1246.

6 (*a*) Y. Imai, K. Kawaguchi, T. Sato, N. Tajima, R. Kuroda and Y. Matsubara, *Mol. Cryst. Liq. Cryst.*, 2008, **487**, 153–159; (*b*) F. P. A. Fabbiani, S. Bergantin, A. Gavezzotti, S. Rizzato and M. Moret, *CrystEngComm*, 2016, **18**, 2173–2181; (*c*) A. L. Litvinov, D. V. Konarev, A. Y. Kovalevsky, I. S. Neretin, Y. L. Slovokhotov, P. Coppens and R. N. Lyubovskaya, *CrystEngComm*, 2002, **4**, 618–622; (*d*) D. V. Konarev, A. L. Litvinov, A. Y. Kovalevsky, N. V. Drichko, P. Coppens and R. N. Lubovskaya, *Synth. Met.*, 2003, **133–134**, 675–677; (*e*) A. A. Sonina, A. D. Kuimov, N. A. Shumilov, I. P. Koskin, T. Y. Kardash and M. S. Kazantsev, *Cryst. Growth Des.*, 2023, **23**, 2710–2720; (*f*) A. A. Sonina, D. S. Cheshkina and M. S. Kazantsev, *Crystals*, 2023, **13**, 861.

7 (*a*) Y. Aoyama, K. Endo, K. Kobayashi and H. Masuda, *Supramol. Chem.*, 1994, **4**, 229–241; (*b*) K. Endo, T. Sawaki, M. Koyanagi, K. Kobayashi, H. Masuda and Y. Aoyama, *J. Am. Chem. Soc.*, 1995, **117**, 8341–8352; (*c*) Y. Aoyama, K. Endo, T. Anzai, Y. Yamaguchi, T. Sawaki, K. Kobayashi, N. Kanehisa, H. Hashimoto, Y. Kai and H. Masuda, *J. Am. Chem. Soc.*, 1996, **118**, 5562–5571.

8 K. Watanabe, T. Toya, Y. Toyota, Y. Kobayashi, J. Usuba, Y. Hijikata, R. Matsuda, K. Nishimura, H. Sugiyama and Y. Segawa, *Chem. Commun.*, 2025, **61**, 2822–2825.

9 M. J. Frisch, G. W. Trucks, H. B. Schlegel, G. E. Scuseria, M. A. Robb, J. R. Cheeseman, G. Scalmani, V. Barone, G. A. Petersson, H. Nakatsuji, X. Li, M. Caricato, A. V. Marenich, J. Bloino, B. G. Janesko, R. Gomperts, B. Mennucci, H. P. Hratchian, J. V. Ortiz, A. F. Izmaylov, J. L. Sonnenberg, D. Williams-Young, F. Ding, F. Lipparini, F. Egidi, J. Goings, B. Peng, A. Petrone, T. Henderson, D. Ranasinghe, V. G. Zakrzewski, J. Gao, N. Rega, G. Zheng, W. Liang, M. Hada, M. Ehara, K. Toyota, R. Fukuda, J. Hasegawa, M. Ishida, T. Nakajima, Y. Honda, O. Kitao, H. Nakai, T. Vreven, K. Throssell, J. A. Montgomery, Jr., J. E. Peralta, F. Ogliaro, M. J. Bearpark, J. J. Heyd, E. N. Brothers, K. N. Kudin, V. N. Staroverov, T. A. Keith, R. Kobayashi, J. Normand, K. Raghavachari, A. P. Rendell, J. C. Burant, S. S. Iyengar, J. Tomasi, M. Cossi, J. M. Millam, M. Klene, C. Adamo, R. Cammi, J. W. Ochterski, R. L. Martin, K. Morokuma, O. Farkas, J. B. Foresman and D. J. Fox, *Gaussian 16, Revision C.02*, Gaussian, Inc., Wallingford CT, 2016.

10 A. D. Becke, *J. Chem. Phys.*, 1993, **98**, 5648–5652.

11 C. Lee, W. Yang and R. G. Parr, *Phys. Rev. B: Condens. Matter Mater. Phys.*, 1988, **37**, 785–789.

12 E. R. Johnson, S. Keinan, P. Mori-Sánchez, J. Contreras-García, A. J. Cohen and W. Yang, *J. Am. Chem. Soc.*, 2010, **132**, 6498–6506.

13 J. Contreras-García, E. R. Johnson, S. Keinan, R. Chaudret, J.-P. Piquemal, D. N. Beratan and W. Yang, *J. Chem. Theory Comput.*, 2011, **7**, 625–632.

14 P. R. Spackman, M. J. Turner, J. J. McKinnon, S. K. Wolff, D. J. Grimwood, D. Jayatilaka and M. A. Spackman, *J. Appl. Crystallogr.*, 2021, **54**, 1006–1011.